8

Limiting Efficiency of Quantum Dot Sensitized Solar Cells: A Detailed Balance Study

8.1 Introduction

The experimental and theoretical efforts are made continuously for the development of photovoltaic devices. Apriori estimation of efficiencies is a key aspect for the development of photovoltaics because apriori theoretical understanding may provide us the possible window of improvement for respective photovoltaic device. Several efforts are made to calculate empirical and theoretical efficiencies for Si based solar cells [Henry, 1980], [Rose, 1960], [Redfield, 1980]. Detailed balance efficiency was calculated by Shockley and Queisser to estimate theoretical limit of Si based single junction solar cells using following assumptions: (i) photons with energy equal or greater than bandgap are absorbed by absorbing material, (ii) one electron and hole pair is generated after absorption of one photon, (iii) solar cell is in detailed balance with its surrounding implying that rate of radiative recombination is equal to rate of absorption of photon from surrounding, and (iv) radiative recombination is a dominant mechanism for recombination [Shockley and Queisser, 1961].

Quantum Dot Sensitized Solar Cells have been investigated intensively in last decade and achieved efficiencies close to 12 % similar to their counterpart Dye Sensitized Solar Cells [Du et al., 2016]. In 2006, Klimov have done detailed balance calculation to estimate detailed balance efficiency limit for Quantum Dot Solar Cell (QDSC) using ideal electron and hole transport material [Klimov, 2006]. They showed that with carrier multiplication, detailed balance limit for a single junction solar cell can be surpassed by QDSC. However, practical QDSSCs are far from ideal ones. They use electron transport material with finite conduction band minima and hole transport material with finite electrochemical potential. These finite values of conduction band minima and finite electrochemical potential decide the highest open circuit voltage [Cahen et al., 2000].

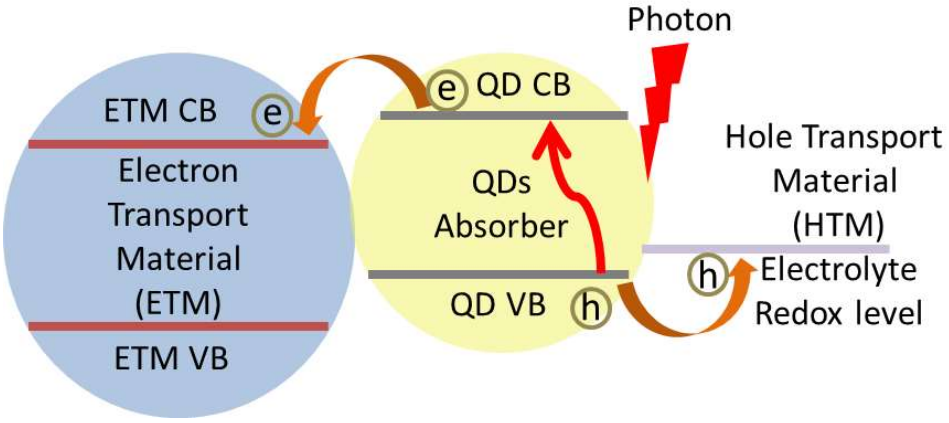

Figure: 8.1 Schematic diagram showing operating principle of QDSSCs.

Figure 8.1 shows schematic diagram of QDSSC operating principle. After absorption of incident photon of energy higher than the bandgap energy, Coulombic bound electron and hole pair exciton is created. Photo-generated electron is injected to electron transport material and hole is captured by hole transport material and finally collected at respective selective contacts for external circuit.

The present study aims to estimate theoretical efficiency of quantum dot sensitized solar cells using detailed balance consideration for practical electron transport material and electrolyte chemical potentials. In ideal electron and hole transport materials, open circuit voltage is determined by the bandgap of QDs absorber and radiative recombination in QDSSCs is considered only. With non-ideal electron and hole transport materials, open circuit voltage is limited and decided by the conduction band minima of electron transport material and finite electrochemical potential of red-ox hole conductor under widely accepted kinetic model of QDSSCs [Cahen et al., 2000]. Open circuit voltage of QDSSCs depends upon quasi Fermi level of electron and hole in electron and hole transport materials, respectively. Cahen et al. estimated that quasi Fermi level of injected electrons will not be higher than the conduction band minima of electron transport material. We considered the difference between conduction band minima of electron transport material normally TiO_2 and red-ox potential of hole conductor normally polysulfide electrolyte as the highest open circuit potential for the solar cell. This difference is denoted as E_{diff}. We also assumed that QDs are in direct contact with electron and hole transport materials. Radiative recombination in QDs and non-radiative recombination between electron and hole transport materials is considered. Multi particle Auger recombination is not considered due to availability of less number of electron and hole pair in QDs as reported by Klimov [Klimov, 2006]. μ_c and μ_v are quasi conduction and valence band potential. The open circuit voltage V is related to quasi conduction and valence band potential as $eV_{oc} = \mu_c - \mu_v$ where e is electronic charge. We also considered that difference between valence band and conduction band is higher than thermal energy available at normal ambient conditions.

8.2 Calculation of Ultimate Efficiency

A photovoltaic device efficiency is limited by ultimate efficiency that employ photovoltaic principle for operation. For calculation of ultimate efficiency, it is considered that all incident photons having energy equal to or higher than bandgap energy of absorber will be absorbed. The rate of incident photons per unit area per unit time can be calculated as $G = \gamma_s \int_{\omega_g}^{\infty} F_s(\omega) d\omega$ where $F_s(\omega) = \frac{\omega^2}{4\pi^2 c^2 (e^{\frac{\hbar\omega}{kTs}} - 1)}$ is the solar photon fluence per unit frequency, ω_g is cut off frequency corresponding to QD bandgap (E_g), γ_s (2.16×10^{-5}) is the dilution factor for earth, T_s is temperature of Sun (5778 K), ħ is reduced Plank constant ($1.054571800\times10^{-34}$ m^2 kg s^{-1}), c is the speed of light (2.99792458×10^8 ms^{-1}), ω is angular frequency of incident photon and K_B is Boltzmann constant (1.38064852×10^{-23} m^2 kg s^{-2} K^{-1}). Since we have considered that all incident photons will be absorbed by QDs absorber this G can be considered as generation rate for electron and hole pairs in QDs absorber. The maximum photon energy in solar flux is considered to be 4.428 eV as reported earlier [Hanna and Nozik, 2006]. Each absorbed photon with energy E_g will produce an electron at an ideal cell voltage $V_g = E_g/q$ for ideal ETM and HTM in QDSSCs. Thus, the output power for ideal QDSSC will be $P_{out} = E_g \times G$ and ultimate efficiency will be $\eta = (E_g \times G)/P_{in}$, where P_{in} is the total incident energy, given as $P_{in} = \gamma_s \int_0^{\infty} F_s(\omega)\, \hbar\omega\, d\omega$; where all the symbols are explained earlier.

Figure 8.2(a) shows generation rate G as a function of absorber bandgap. Generation rate shows exponential decay with increasing absorber bandgap. Ideal ultimate efficiency for an ideal QDSSC is plotted in Figure 8.2 (b). It is similar to the one predicted by Klimov [Klimov, 2006]. For practical QDSSCs, open circuit potential is limited by conduction band minima and redox electrolyte and it is equal to E_{diff}. So for practical QDSSC with non-ideal ETM and HTM, each absorbed photon energy with E_g or higher will produce electron with cell voltage V that cannot be higher than E_{diff}. In this study, we have considered titanium oxide as electron transport material and polysulfide electrolyte hole conductor as hole transport material. Unless specified, value of E_{diff} is considered to be 0.8 eV. So for non-ideal case, output power will be $P_{out}=E_{diff}\times G$ and ultimate efficiency will be $\eta = (E_{diff}\times G)/P_{in.}$

Calculated ultimate efficiency is shown in Figure 8.2 (b). It is observed that the maximum ultimate efficiency for an ideal QDSSC is 44 % near 1.1 eV absorber bandgap similar to earlier reports. We observed that this maximum in ultimate efficiency is shifted close to E_{diff} for limited V_{oc} case and decrease exponentially for higher absorber bandgap similar to the generation rate. As evident from definition of ultimate efficiency for non-ideal case, it is just a scaled version of the generation rate and that's why the exponential decay similar to that in case of generation rate is visible. Ideal ultimate efficiency is function of absorber bandgap and generation rate and thus, ultimate efficiency attains the maximum value close to 1.1 eV, with a slow decay with bandgap.

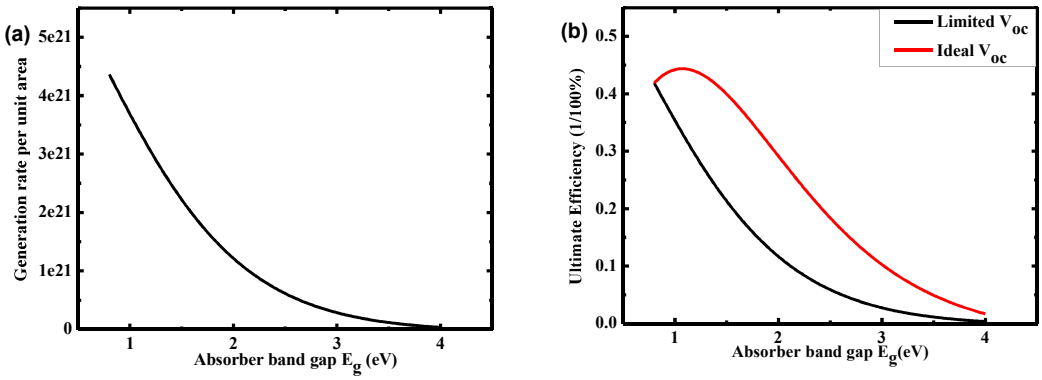

Figure: 8.2 (a) Generation rate and (b) ultimate efficiency for limited V_{oc} and ideal V_{oc} case.

8.3 Calculation of Ultimate Efficiency with Carrier Multiplication

Quantum Dots are supposed to have efficient carrier multiplication, so the effect of carrier multiplication is studied on ultimate efficiency. In carrier multiplication, more than one electron-hole pair generation is possible with absorption of one photon. So carrier multiplication affects generation of electron-hole pair i.e. generation rate. To include effect of carrier multiplication in generation rate, internal quantum efficiency IQE(ω) is introduced in generation term. Earlier, it was considered that one electron and hole pair will be generated after absorbing one photon, so IQE(ω) is considered to be 100 %. For carrier multiplication enhanced ultimate efficiency G′ is defined as $G' = \gamma_s \int_{\omega_g}^{\infty} IQE(\omega)F_s(\omega)d\omega$ and this CM enhanced generation rate is used in further calculation of ultimate efficiency as discussed in section 8.2.

Two cases of carrier multiplication (CM) are considered for ultimate efficiency. The first one is ideal carrier multiplication, showing stair case behavior, defined as IQE(ω) = U(E-E_g) + U(E-2E_g) + U (E-3E_g) + ……; where U is unit step function and E_g is absorber bandgap, Figure 8.3 (a). In second case, a finite CM threshold is considered that depends upon effective mass of carriers followed by finite slope CM. In this study, this finite slope CM is considered for PbSe QDs as considered by Klimov earlier [Klimov, 2006] and it is defined as IQE (ω) = U(E-E_g) + slope(E- Eg_$CM_{threshold}$) U(E- Eg_$CM_{threshold}$), considering CM threshold in PbSe QDs as (E_g_$CM_{threshold}$) = 2.85 E_g, followed by a linear slope of 1.14/E_g, as reported for PbSe QDs with E_g = 0.8 eV [Richard D. Schaller et al., 2006]. This case of carrier multiplication is plotted in Figure 8.3 (b).

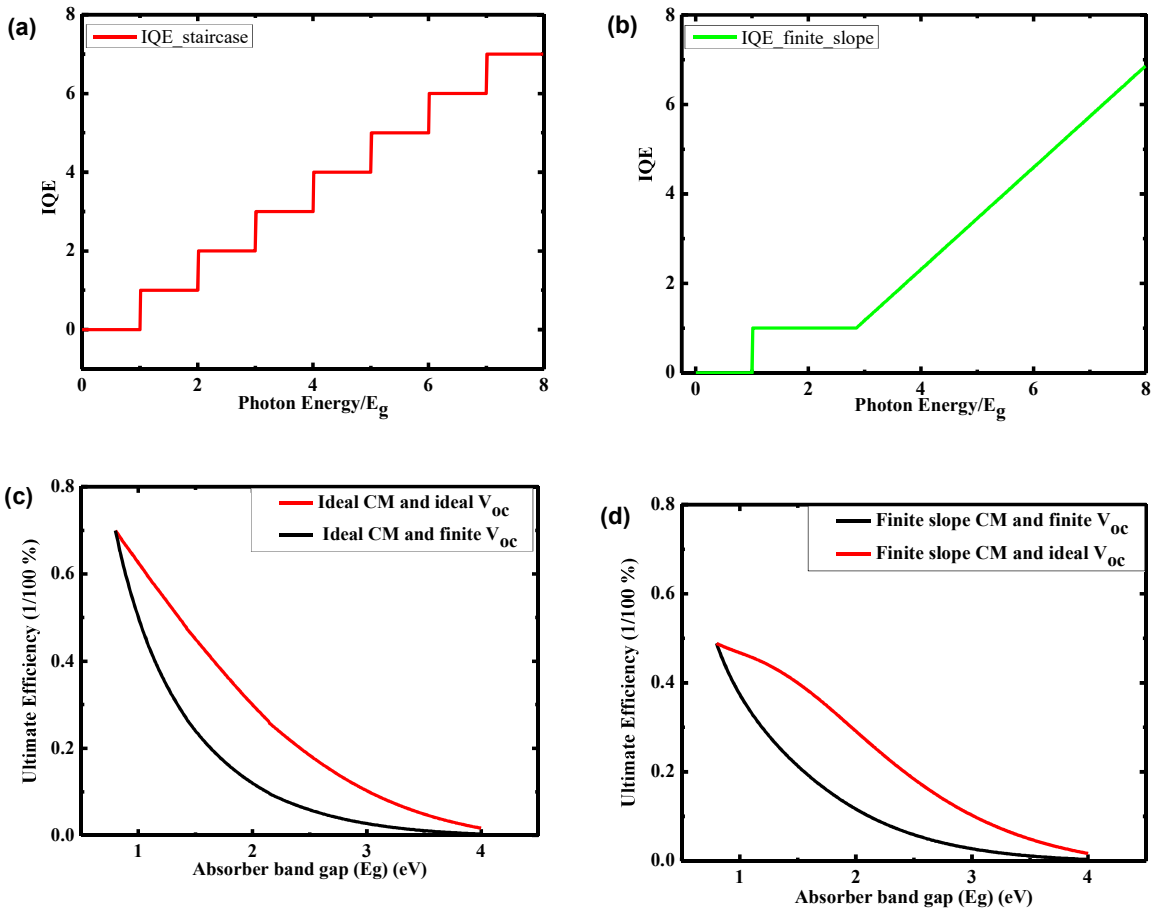

Figure: 8.3 (a) Staircase carrier multiplication, (b) finite slope carrier multiplication, (c) ideal ultimate efficiency and non-ideal ultimate efficiencies for staircase carrier multiplication and (d) ideal and non-ideal ultimate efficiency for finite slope carrier multiplication.

Figure 8.3 (c) shows ideal ultimate efficiency and non-ideal ultimate efficiency for staircase carrier multiplication and finite slope carrier multiplication. We found ultimate efficiency as high as 70 % for staircase carrier multiplication in case of ideal ETM and HTM. This ultimate efficiency shows decay with increasing absorber bandgap and does not hit a maximum as earlier. So, it was concluded that carrier multiplication effect dominates increasing

photo voltage with increasing band gap and efficiency decrease with increasing absorber bandgap as number of photons become less for carrier multiplication. For finite V_{oc} case and stair case carrier multiplication, it decreases rapidly under the influence of decreasing generation rate with higher absorber bandgap and finite E_{diff}.

We observed that ultimate efficiency for a finite slope CM starts from the maximum 50 % in contrast to 70 % for ideal carrier multiplication for both ideal ETM and HTM case and finite V_{oc} case. In this case, we don't see a sharp decrease in ultimate efficiency for ideal ETM and HTM. The increasing bandgap is showing its effect on ultimate efficiency as effect of carrier multiplication is reduced. But for limited V_{oc} case, the ultimate efficiency has decreased below 10% for E_g values greater than 2 eV, Figure 8.3 (d).

8.4 Calculation of Detailed Balance Efficiency for QDSSCs

Following assumptions are made to calculate current –voltage characteristic for QDSSC: (i) number of QDs are sufficient to absorb all incident photons having energy equal or higher to the absorber bandgap, (ii) each photon with energy equal or above bandgap is converted to one e-h pair, and (iii) rate of radiative recombination in dark is equal to rate of absorption of photon from ambient i.e. device is in detailed balance with its surrounding. Photogenerated carrier generation equation is written by setting net extracted current equal to the difference between net generation and net recombination of carriers considering both radiative and non-radiative cases [Shockley and Queisser, 1961]. Thus, rate of carrier extraction per unit area can be given as $I = e\left[G + F(E_{diff}) - F(E_g)e^{\frac{eV}{kT}} - F(E_{diff})e^{\frac{eV}{kT}}\right]$, where G is generation rate of electron and hole pair by absorption of incident of solar radiation. Radiative recombination between electron and hole in QDs absorber is $F(E_g)\ e^{eV/kT}$ and it is proportional to the product of electron and hole population. It also depends on quasi Fermi levels of electron and hole, hence cell voltage V. $F(E_g)$ is radiative recombination coefficient and depends on quantum dot bandgap which comes from the detailed balance condition. Radiative recombination is considered to take place in QDs absorber while non-radiative recombination is considered to take place between electron transport material and hole transport material mediated by various defect states in nanostructured materials [Hodes, 2008]. Non-radiative generation term is $F(E_{diff})$ that depends upon energy difference between conduction band minima of electron transport material and electrochemical potential of redox electrolyte. Ambient temperature T is 300K and $F(E_{diff})e^{\frac{eV}{kT}}$ is non radiative recombination term between electron and hole transport materials. V is the voltage difference between quasi Fermi level of electron and hole between terminals of photovoltaic device. $F(E_g)$ is defined as $F_e = 2\int_{wg}^{\infty} F_a(\omega)d\omega$; where 2 specify black body radiation from both side of the solar cell, thus increasing the surface by a factor of 2, as considered in earlier reports [Shockley and Queisser, 1961]. Under detailed balance, it is considered that rate of radiative recombination will be equal to rate of absorption of photons from ambient. Photon fluence of black body at room temperature is $F_a(\omega)$. The QDSSC current per unit area can be calculated as $I = e\frac{dN_{eh}}{dt}$, where e is electronic charge. Thus, current – voltage characteristic for QDSSC can be given as $I = e\left[G + F(E_{diff}) - F(E_g)e^{\frac{eV}{kT}} - F(E_{diff})e^{\frac{eV}{kT}}\right]$. The open circuit voltage V_{oc} is defined as the difference between quasi Fermi levels of carriers in equilibrium, for which current I is 0. Thus, for I=0, open circuit potential relation will be given as $eV_{oc} = kT_a \log_e \frac{G+F(E_{diff})}{F(E_g)+F(E_{diff})}$.

Non radiative recombination term $F(E_{diff})$ is calculated under assumption that at 0 K surrounding temperature, there will be no radiative recombination and open circuit voltage will be equal to its maximum value i.e. E_{diff}. Following this assumption, $F(E_{diff})$ is defined as

$F(E_{diff}) = G/(e^{\frac{E_{diff}}{E_T}} - 1)$; where E_T is equivalent thermal energy at ambient temperature T_a defined as kT_a/e and G is generation rate, as defined above.

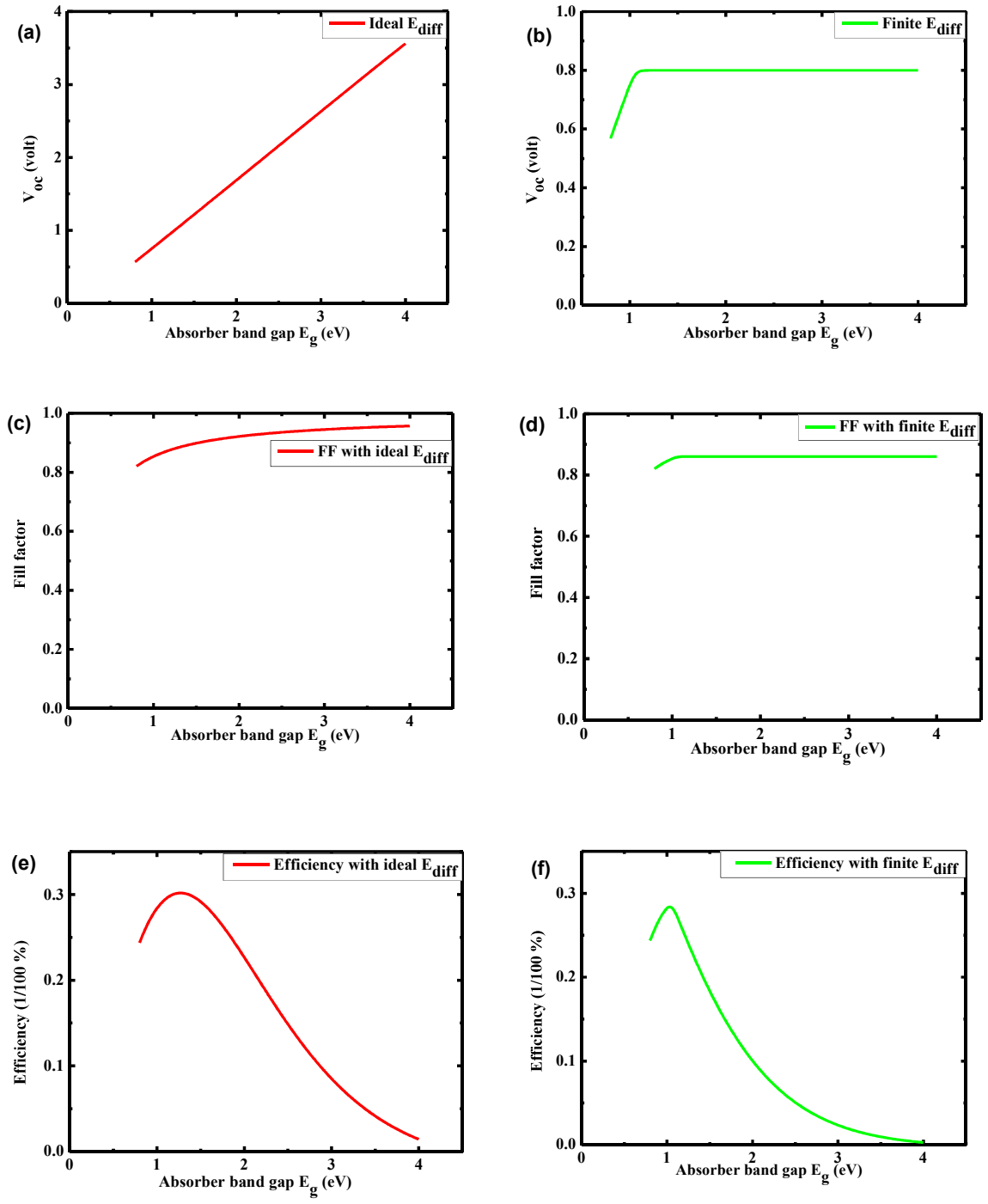

Figure: 8.4 (a) open circuit voltage, (c) fill factor, (e) detailed balance efficiency with ideal E_{diff}, (b) open circuit voltage, (d) fill factor and (f) detailed balance efficiency with finite E_{diff}

Two different approximations are considered for calculation of photovoltaic performance. In first approximation, ideal electron and hole transport material are considered i.e. E_{diff} is equal to bandgap of absorber. In second approximation, finite E_{diff} is considered equal to 0.8 eV. These current-voltage relations are solved to find device performance parameter. Open circuit voltage is calculated as stated above and fill factor is calculated by finding the maximum of extracted power divided by product of short circuit current density and open circuit voltage.

In Figure 8.4 (a) and (b), open circuit potential against absorber bandgap is plotted for ideal E_{diff} and finite E_{diff} cases, respectively. We observed that for ideal E_{diff} case, V_{oc} increase with absorber bandgap while for finite E_{diff} case, V_{oc} does not increase above 0.8 Volt as discussed above. V_{oc} increases for initial increase in bandgap and approach the maximum value at absorber bandgap 1.1 eV but after that it does not increase for higher bandgap. Figures 8.4 (c) and 8.4 (d) show fill factor against absorber bandgap for ideal E_{diff} and finite E_{diff} cases, respectively. For an ideal E_{diff} case, fill factor increases gradually with absorber bandgap while for finite E_{diff} case, fill factor increases initially with bandgap and reaches a maximum value at absorber bandgap 1.08 eV and does not show increase for higher bandgap values. Figures 8.4 (e) and 8.4 (f) show detailed balance efficiency for ideal E_{diff} and limited E_{diff} cases, respectively. Figure 8.4(e) shows a well reported bell shaped curve for ideal E_{diff} case. It shows 30 % highest efficiency at 1.27 eV absorber bandgap for ideal E_{diff} case but this bell shape curve get narrow and higher reduction rate is noticed for higher absorber bandgap, Figure 8.4 (f). It shows the maximum efficiency of 28 % for absorber bandgap ~ 1 eV but much steeper reduction in efficiency for higher bandgap absorber can be seen. The maximum efficiency values are at different bandgap values of QDs absorber for both cases. With limited E_{diff}, close to 1 eV absorber bandgap the maximum efficiency is noticed. V_{oc} and FF are limited to their maximum values and do not show any enhancement with increasing QD absorber bandgap values, whereas these keep on increasing with increasing absorber bandgap for ideal E_{diff} case. This might be the reason for having the maximum efficiency at different absorber bandgap in both cases.

8.5 Calculation of Detailed Balance Efficiency for QDSSCs with Carrier Multiplication

To estimate detailed balance efficiency under the influence of carrier multiplication, two cases of carrier multiplication are considered. First one is staircase carrier multiplication and second is finite slope carrier multiplication with finite threshold as discussed in section 8.3. Carrier multiplication modified generation terms are used in calculation of device performance parameters and detailed balance efficiency as discussed in sections 8.3 and 8.4, respectively. Open circuit voltage for stair case carrier multiplication and finite slope carrier multiplication are shown in Figures 8.5 (a) and 8.5 (b), respectively. For ideal carrier multiplication, open circuit voltage increases till absorber bandgap ~ 1 eV and saturates afterwards. This trend in open circuit voltage is similar for finite slope carrier multiplication. It shows that impact of carrier multiplication is less on open circuit voltage under detailed balance consideration as compared to the impact of finite E_{diff}. Fill factor for stair case carrier multiplication and finite slope carrier multiplication are shown in Figures 8.5 (c) and 8.5 (d), respectively. For ideal carrier multiplication, fill factor increases till ~1 eV absorber bandgap and saturates afterwards. It shows that impact of carrier multiplication is also less on fill factor under detailed balance consideration as compared to the impact of finite E_{diff}. Detailed balance efficiencies are plotted in Figures 8.5 (e) and 8.5 (f) under ideal and finite slope carrier multiplications. The maximum detailed balance efficiency is 42 % at absorber bandgap equal to E_{diff} and decrease slowly till 0.98 eV bandgap. This is associated with increase in fill factor and open circuit voltage till 1 eV absorber bandgap. Detailed balance efficiency decrease rapidly after 1 eV bandgap. Figure 8.5 (f) shows detailed balance efficiency in case of finite slope CM. The maximum efficiency is 30 %

for 1 eV absorber bandgap with finite slope CM which starts decreasing for higher absorber bandgap. This relatively less efficiency as compared to staircase CM case is attributed to the lower impact of carrier multiplication with higher threshold and finite slope.

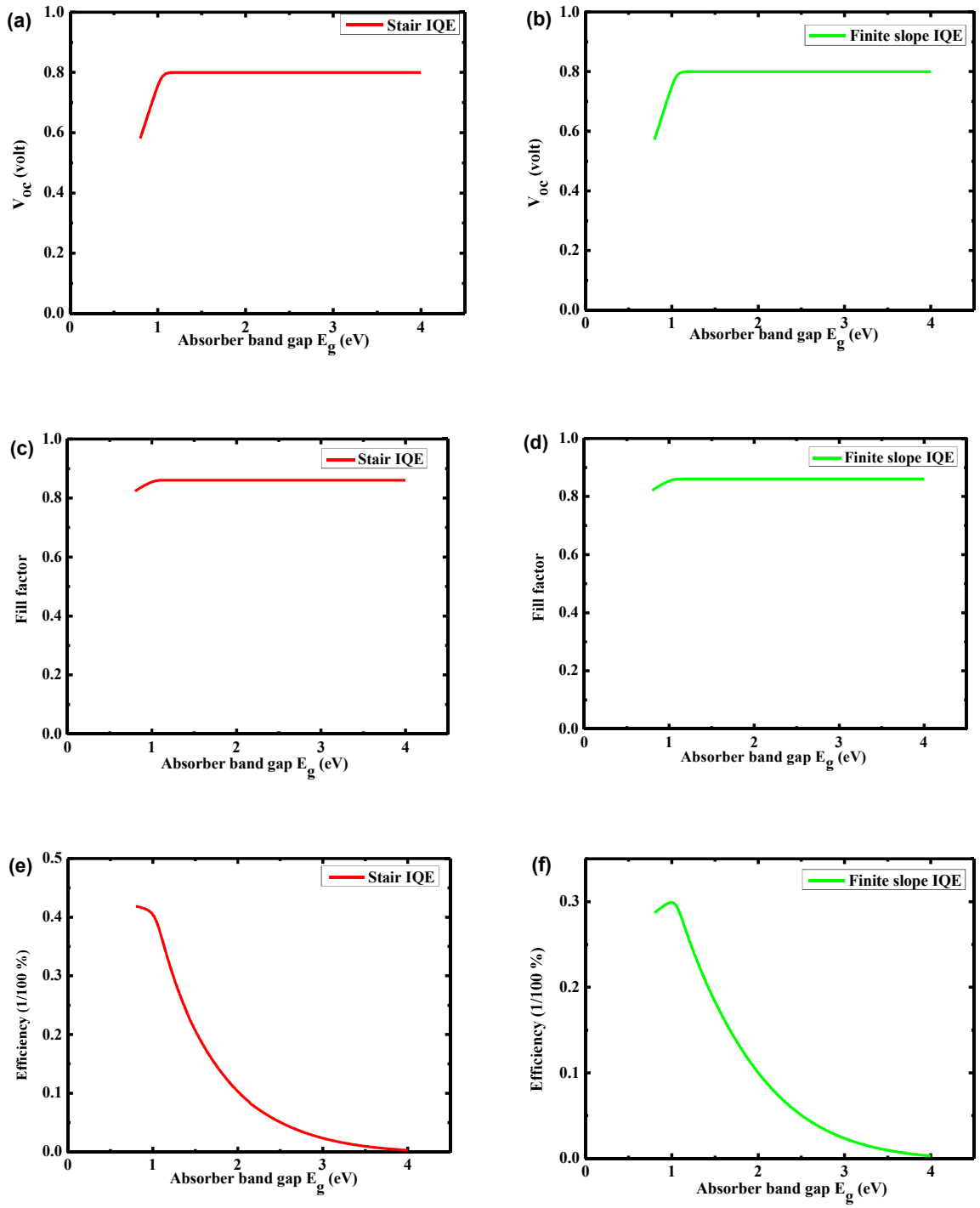

Figure: 8.5 (a) open circuit voltage, (c) fill factor, (e) detailed balance efficiency with finite E_{diff} and staircase carrier multiplication, (b) open circuit voltage, (d) fill factor and (f) detailed balance efficiency with finite E_{diff} and finite slope carrier multiplication

However, variation in efficiency is similar for staircase carrier multiplication and finite slope carrier multiplication with finite threshold for higher absorber bandgaps. For stair case carrier multiplication, the highest efficiency is 42 %, which is about 30 % for finite slope CM case. These efficiency values are similar to Klimov's work [Klimov, 2006]. However, for higher bandgap, the detailed balance efficiency values are relatively lower than predicted by Klimov for ideal electrodes. For example, detailed balance efficiency without CM is close to 20 % for absorber bandgap close to exciplex quantum dots [Jiao, Shen, Mora-Seró, et al., 2015] while Klimov predicted detailed balance efficiency as high as 30 %. The detailed balance efficiency predicted under finite E_{diff} cases are more close to the experimental observations than efficiencies predicted for ideal E_{diff} case. These studies suggest that finite value of ETM and HTM levels affect QDSSCs efficiency significantly as compared to that of the ideal ETM and HTM case, especially in the higher bandgap region. Further, even with the presence of carrier multiplication, there is no drastic increase in detailed balance efficiency of QDSSCs.

8.6 Concluding Remarks

The present work demonstrates that the detailed balance efficiency for QDSSCs depends strongly on finite energy level difference between electron and hole transport material. This difference hampers efficiencies for higher absorber bandgap values. Carrier multiplication with finite slope and finite threshold is also less effective for higher bandgap absorber showing design limitations for QDSSCs.

...